www.cadanda.com
Computer-Aided Design AND APPLICATIONS

Multi-objective Topology Optimization with Ant Colony Optimization and Genetic Algorithms

João Batista Queiroz Zuliani[1], Miri Weiss Cohen[2], Lucas de Souza Batista[3] and Frederico Gadelha Guimarães[4]

[1]Centro Federal de Educação Tecnológica de Minas Gerais, joao@timoteo.cefetmg.br
[2]ORT Braude College of Engineering, miri@braude.ac.il
[3]Universidade Federal de Minas Gerais, lusoba@ufmg.br
[4]Universidade Federal de Minas Gerais, fredericoguimaraes@ufmg.br

ABSTRACT

In this work, we present a multi-objective approach for Topology Optimization applied to the design of devices with several materials. The first stage consists of applying a Multi-Objective Ant Colony Optimization (MOACO) to find tradeoff topologies with different material distributions. In the second stage, we parameterize the boundaries of the topologies found by using NURBS. A Multi-objective Genetic Algorithm is applied as a heuristic optimization engine to optimize the control points, weights and knots of the curves in order to smooth and refine the boundaries of the topology. The main advantage of a multi-objective approach is that the designer can identify, explore and refine a number of tradeoff topologies. The proposed methodology is illustrated in the design of a C-core magnetic actuator.

Keywords: topology optimization, NURBS, ant colony, genetic algorithms.

1. INTRODUCTION

Topology Optimization (TO) [2–5], [18] is a design process by which new designs can be explored by optimally distributing material in the design region. The best designs are achieved according to the objectives and constraints defined for the specific application. Since pioneering works by Bendsoe and Kikuchi [4], Topology Optimization methods have been applied to various physical systems, including electromagnetic devices and machines [2,3],[18].

Lin e Chao [15] presented an integrated approach that supports structural topology and shape optimization. First they employ homogenization or material distribution methods. After that, the generated gray level image is converted to a parameterized structural model by means of an image interpretation method. Finally, a shape optimization is performed to get a fine-tuned configuration, ensuring satisfaction of all design constraints. The integration is carried out by first converting the geometry of the topologically optimized structure into smooth and parametric B-spline curves and surfaces. This conversion is made by using template matching. Then the B-spline curves and surfaces are imported into a parametric CAD environment to build solid models of the structure. The control point movements of the B-spline curves or surfaces are defined as design variables for shape optimization, in which CAD-based design velocity field computations, design sensitivity analysis (DSA), and nonlinear programming are performed. The interpretation of the gray level image created at the first stage is the main limitation of this proposal.

Tang and Chang [19] proposed an integrated design approach that has been demonstrated to be feasible for structural optimization. The approach consists of five main steps: design problem definition; topology optimization using the homogenization method or the Solid Isotropic Microstructure with Penalty (SIMP) method; boundary smoothing techniques; geometric reconstruction in Computer-Aided Design (CAD) solid model form; and CAD-based shape optimization. The integration is carried out by first converting the geometry of the topologically optimized structure into smooth and parametric B-spline curves and surfaces. The proposed solid model generation method requires significant user interactions and decisions, especially when branches are involved. Another drawback is that mesh distortions can occur, making the batch mode shape optimization impossible.

Taylor & Francis
Taylor & Francis Group

Campelo et al. [5] presented a hybrid methodology for the design of electromagnetic devices that employs a Clonal Selection algorithm for Topology Optimization (TopCSA) in order to obtain an initial design for a given device under consideration, followed by an automatic generation of a parametric model by means of image processing technique. The shape optimization is performed with the Real-coded Clonal Selection Algorithm using the control points for the refinement and improvement of the design solution.

Heo et al. [11] integrated shape and topology optimization in the design of the rotor of a synchronous reluctance motor (SynRM), using the sensitivity analysis along with the level set method. Automated methods for Topology optimization and CAD are discussed in [7,8], [14]. The optimization of parameterized CAD models is studied in [17]. More studies on the integration between topology and shape optimization can be found in [12,13].

An important limitation of previous studies is dealing with one material (presence or absence of material in the design region). In contrast to these studies in the literature, we describe herein an integrated topology and shape optimization approach that can deal with multi-objective problems and multi-material designs.

The methodology to represent the design region as a grid and the allocation of material as a graph in this grid was first proposed in [2] for single objective problems. This allows the representation of the TO problem with multiple materials in a very simple way. In addition, this reduces the topology optimization to a problem of finding an optimal route in the graph. Ant Colony Optimization (ACO) is a very efficient heuristic for such a task and was applied to solve mono-objective problems [2]. However, this methodology in most cases results in a non-smooth topology, which is not desirable in most of industry applications.

In this paper, we present an automated and integrated multi-objective approach for topology and shape optimization, using multi-objective evolutionary algorithms. The first stage consists of applying a multi-objective Ant Colony Optimization (MOACO) to find tradeoff topologies with different material distributions. In the second stage, we parameterize the boundaries of the topologies found by using NURBS. Multi-objective genetic algorithms are applied as a heuristic optimization engine to optimize the control points of the curves in order to smooth and refine the boundaries of the topology. The main advantage of this multi-objective approach is that the designer can identify, explore and refine a number of tradeoff topologies. Extending it to a multi-objective context makes the solution of topology optimization much more flexible and easier from the designer perspective. The shape optimization step using genetic algorithms will be held to overcome the low smoothness and some numerical instabilities usually obtained by the results of the Multi-Objective Ant Colony Optimization (MOACO). In order to have more flexibility in handling the boundaries of the topologies in the parameterized model, Non-Uniform Rational B-Spline (NURBS) will be used. The methodology is illustrated in the design of a c-core magnetic actuator. The results show the adequacy of the proposed approach to topology optimization.

2. MAIN BODY

The design region of a Topology Optimization problem is represented by a finite and bounded d-dimensional subset $\Omega \subset \mathbb{R}^d$, with $d = 2$ or 3, in which $c \in \Omega$ denotes a cell within this geometric space. Each cell c is associated with one out of n possible states. By considering the state of a given cell as the material properties at that point, then the general multi-objective TO problem can be defined as finding the optimal distribution of material in the cells of the design region that minimizes the objective functions while satisfying the problem constraints, which are mathematical representations of the system requirements and limitations.

In the proposed approach we extend the ACO method proposed in [2] to solve multi-objective topology problems. Although there are a number of studies on using genetic algorithms for topology optimization, the definition of a suitable representation for the genome and genetic operators is very cumbersome. With ACO, we can represent the design region as a grid and the allocation of material as a graph in this grid, thus reducing the topology optimization to a problem of finding an optimal route in this graph. The resulting topologies represent tradeoff topology designs, more precisely, approximations of the Pareto-optimal solutions of the multi-objective TO problem. These topologies are coarse initial designs, that should be smoothed and refined, nonetheless, the designer can have a first overview of the design possibilities.

Next, when the designer chooses one topology from the tradeoff set, we identify the boundaries of the regions with different materials by using a boundary detection algorithm. The points along each boundary are used to fit and define a NURBS curve for that boundary. The control points, the knots and weights of the NURBS curves are then optimized by means of multi-objective GA, using the same objective and constraint functions of the original problem, but in a different search space. In this way, another set of tradeoff solutions is generated around the topology chosen by the designer. This new Pareto front represents possible refinements of the initial coarse topology identified in the previous stage.

The final design can be selected out of the tradeoff solutions by using any decision-making methodology. The designer can go back to the solutions identified in the first stage, select another topology from this

set and perform the NURBS parameterization and GA optimization on this topology, in order to analyze other design alternatives.

In the next sections the main steps of the suggested approach to the topology and shape optimization will be detailed.

2.1. Ant Colony Optimization

The Ant Colony Optimization (ACO) was introduced by M. Dorigo in 1992 and has been used to solve many combinatorial optimization problems, including multi-objective ones [20]. It is based on the foraging behavior of some real ants that deposit pheromone along their paths when returning to their nest after successfully finding a food source. The path can be used by the other ants and eventually they can find the shortest path between the food source and the nest. Inspired by this behavior, the ACO uses a pheromone model to construct candidate solutions and to bias future sampling towards high quality solutions. Algorithm 1 summarizes the ACO metaheuristic [10].

Figure 1 illustrates the graph representation of the design space to deal with topology optimization problems proposed in [2]. The scheme in Fig. 1 can reduce the topology optimization to a problem of finding an optimal route in the graph, for which the ACO is a very efficient heuristic.

On this graph scheme, each edge, e_l, $l = 1, \ldots, u$ represents a material property on the cell c_{ij} of the topological matrix representation of the discretized design space. In principle, this approach can handle several materials. A route in this graph, representing a valid topology in the design space, is constructed by applying the *AntBasedSolutionConstruct()* routine. The route is performed from the first to the last cell in this directed graph using only one edge in each cell. Note that the nodes of the route are in a fixed order, thus the components of the route are the edges which represent the several available materials

Here, this approach was extended for multi-objective problems and the main difference is the

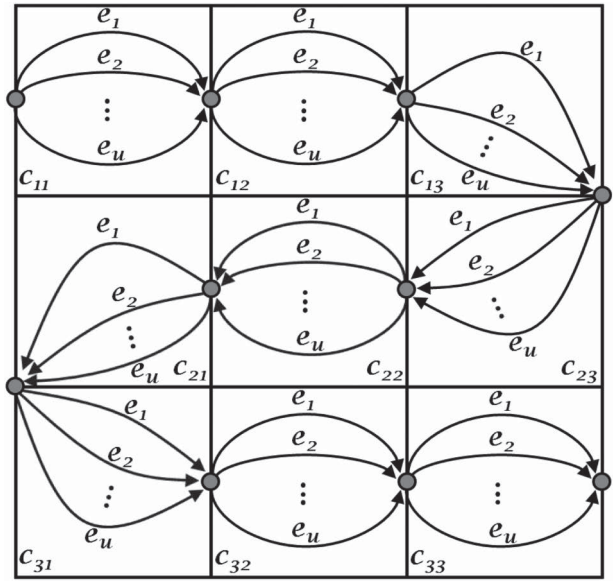

Fig. 1: Graph representation of the design space.

way that the pheromone update occurs. The proposed MOACO can be explained by the flowchart of Fig. 2 that shows the steps detailed bellow:

- **Initialization:** First define the number n_a of ants, the number u of available materials, the maximum number $nc_{\max}$ of cycles that is the stop criterion and the initial value of the pheromone on each edge e_l of the cell c_{ij} as $\tau_{ij}^{e_l} = \tau_0 = \frac{1}{u}$ for all cells of the topological matrix representation. Also the parameters that will be used in the probabilistic rules (α, β and the initial heuristic values η_0) and in the pheromone updating processes (ρ, Q, $r_{\max}$) are provided. Another input data should be the structure that represents the discretized design space in the combinatorial optimization problem (COP) model. In this work we have chosen to use one colony and one pheromone structure due to its simplicity and

Algorithm 1: Ant Colony Optimization Metaheuristic

```
1 Input: instance P of a COP
2 begin
3     Initialization of pheromone values, heuristic values. Set parameters;
4     while termination conditions not met do
5         ScheduleActivities;
6             AntBasedSolutionConstruction();
7             DaemonActions() {optional};
8             PheromoneUpdate();
      end
  end
9 Output: The global best solution
```

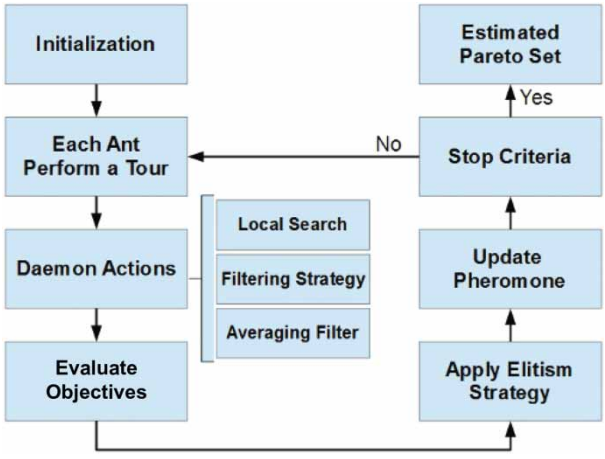

Fig. 2: Flowchart of the proposed MOACO.

to the good results obtained at the experimentations done.

- **AntBasedSolutionConstruct():** Since the graph representation is a directed graph, each ant starts from the first node and makes its tour to the last one. The probability $p_{ij}^{s_p,e_k}$ of the ant s_p to choose the edge (material) e_k on the cell c_{ij} is defined as:

$$p_{ij}^{s_p,e_k} = \frac{\tau_{ij}^{e_k}}{\sum_{e_l \in N(s_p)} \tau_{ij}^{e_l}}, \forall e_k \in N(s_p) \qquad (2.1)$$

where the set $N(s_p)$ is a neighborhood structure which contains the components e_k that once used to extend the solution created by s_p and make this extended solution still feasible. The heuristic information η_0 was not considered in the definition of the probability $p_{ij}^{s_p,e_k}$ such as in other ACO algorithms.

- **Daemon Actions():** Four actions were implemented. The first two, the local search by visibility information and a filtering strategy, are implemented as proposed in [2].
  1. The local search procedure using visibility information was applied at every nc_v cycles. This was done by taking randomly some ant tour (solution) s_p and using its material distribution over the design space (topology) to change the probability of choosing an edge. The new probabilistic rule is defined using the information about the material surrounding each cell c_{ij} and the heuristic value $\eta(c_{il})$ is a positive number that indicates the number of neighbor cells of c_{ij} that have the same material. The new rule is formulated as:

$$p_{ij}^{s_p,e_k} = \frac{\tau_{ij}^{e_k}.[\eta(c_{ij})]^{\beta}}{\sum_{e_l \in N(s_p)} \tau_{ij}^{e_l}.[\eta(c_{il})]^{\beta}}, \forall e_k \in N(s_p) \quad (2.2)$$

  From this particular solution chosen, the *AntBasedSolutionConstruct()* is performed using the probabilistic rule in Eqn. 2.2 where the heuristic values are considered. At the end of the construction, a new solution is created with an expected smoother shape.
  2. The filtering strategy is a simple mean filtering mechanism applied at every n_{fs} over the pheromone matrix with the goal of reducing the amount of trail intensity variation between adjacent cells, and then promoting the generation of smooth topologies.
  3. A third mechanism to enforce smoothness in a different way is applied at every nc_{af} cycles. The mechanism is performed in n_t randomly chosen solutions at the set S_{best} of best solutions found in the current cycle. Then an averaging filter is applied randomly t_1 times over the topology defined by this solution. The averaging filter is performed using a mask 2×2 and changing the materials to the value that appears more often in the mask.
  4. At last, also an elitism strategy was used. After all solution construction and daemon actions are performed, all routes are evaluated. The new solutions are added to those in the set of the global best solutions found S_{gbest} and then the new Pareto ranking is assigned. The best n_{fr} Pareto ranked solutions are stored in an archive with fixed size. If the number of points at the first front is greater than the size of the archive, the crowding distance is used to select which ones will remain at the archive.

- **PheromoneUpdate():** In order to update the pheromone model for the multi-objective TO, the method combines the Pareto dominance depth ranking (considering the ants tour in S_{gbest}) and information about the time the ants were inserted into S_{gbest}. The higher the rank and the longer a solution is in the archive, the smaller is the pheromone increase. In this way, the influence of solutions that are present in S_{gbest} for many iterations is reduced to avoid premature convergence to these solutions. The variation $\Delta\tau_{ij}^{s_p e_l}$ in the quantity of pheromone laid on edge e_l on cell c_{ij} by the ant performing the s_p tour at the end of one iteration is given by

$$\Delta\tau_{ij}^{s_p e_l} = \begin{cases} \frac{r_{\max} - r_{s_p} + 1,}{\min(t_p, 10)} \cdot Q, & if\ e_l \in s_p \\ 0, & otherwise \end{cases} \qquad (2.3)$$

where Q is a positive constant, $r_{\max}$ is the maximum rank allowed for solutions in S_{gbest}, r_{s_p} is the rank of the particular solution $s_p \in S_{gbest}$ and t_p is the time (number of cycles) that the

particular solution s_p is in the archive. If a solution s_p just entered the archive, then we assume that $t_p = 1$. Note that solutions with lower ranks contribute more to increasing the pheromone amount and the longer a solution is in the archive the less it contributes according to Eqn. 2.3. Then the update of the pheromone trail of all components is done by:

$$\tau_{ij}^{e_l} \leftarrow (1-\rho)\tau_{ij}^{e_l} + \sum_{s_p \in S_{gbest}/c_{ij} \in s_p} \Delta\tau_{ij}^{s_p e_l} \qquad (2.4)$$

The parameter ρ is the pheromone evaporation rate. The pheromone trail is normalized and corrected for all values smaller than a lower bound.

- **Stop criterion:** the criterion used was the maximum number of cycles $nc_{\max}$, but other usual criteria are a predefined maximum execution time or when the stagnation behavior of the S_{gbest} is observed.

2.2. Parameterization

The topologies returned by the ACO method can be further parameterized and refined using a Genetic Algorithm. For an efficient parameterization of the curves that define the boundaries between different materials in the topology, we chose to use NURBS. The geometrical characteristics that motivate this choice are:

- Strong convex hull property: a NURBS curve of order p (degree $p-1$) lies within the union of convex hulls formed by p successive control polygon vertices. This provides control about the shape of the curve.
- Local approximation: changes in a control point or in a weight value affects the NURBS curve only locally;
- Smoothness.
- The extreme points are the first and the last control points.

In order to obtain a parameterization of one or more topologies on the non-dominated set identified by the optimization with ACO, we apply the following procedure:

1. Matrix Preprocessing: Cleaning; Surface smoothing; Matrix Refinement;
2. Vertices classification;
3. Map vertices in the representation matrix to Cartesian coordinates in the design region. Select the control points and degree of the NURBS curves;
4. Determination of weights and knots.

In the preprocessing step, the Cleaning operator removes isolated elements, i.e., those without neighbors with the same material property. This works as filtering imperfections over the topology. The surface smoothing operator smoothes the boundaries eliminating some points along the boundary and facilitating the subsequent parameterization. Finally, the Matrix refinement operator increases the matrix resolution. Each element is further divided into k^2 elements. This increases the number of vertices available for selection in the process of defining the control points, hence increasing flexibility.

Given that the main goal in the preprocessing stage is to prepare for the continuous optimization (shape optimization) of the topology of interest, some of the choices made here were done in order to avoid the appearance of new regions and holes. In other words, the topology is fixed and cannot be changed by the genetic algorithm. The topological characteristics of the solution under refinement should not be changed. New regions could appear as a consequence of the intersection of approximating curves in the boundary of two regions with different materials. Therefore, the intersections of curves and the contact with the global boundary of the design region should not be modified during the optimization by the genetic algorithm. This requirement can be satisfied by forcing the intersection points to be the initial or final control points of the curves.

The next step is to define the polygonals that make up the boundaries. After the preprocessing, all edges of the discretized region that are between two cells of different material are identified as belonging to the boundary. Each vertex of the discretized region receives a value from 0 to 4 corresponding to the number of the edges belonging to the boundary that is linked to it. For example, consider a square that was discretized in a grid 3×3 as in Fig. 3 (a). In Fig. 3 (b) the edges identified in red are those that will compose the polygonal that makes up the internal boundaries of the topology. The value 0 is assigned to the vertex P since the two neighboring cells are composed of the same material, the vertex S receives value 1, the vertex Q receives value 2 and the vertex R receives value 3.

The next step is to determine the polygonal that will represent the internal boundaries. In Fig. 3 (c) they are the yellow, green and purple lines. Note that this classification implies that the vertices that are in the intersection of polygonal lines are assigned with values 3 or 4 and the vertices that are on the external boundary of the discretized space are assigned with value 1. After classifying all vertices it is possible to determine the vertices of each polygonal lines (in the representation of the design region) in a way that the first and the last are points with classification 1, 3 or 4, and the other points in the lines have value 2. For simple closed polygonal lines all vertices have value 2 and the list will start and finish on any of these vertices. The vertices with value 0 are not points in the internal boundary. After this classification and choice

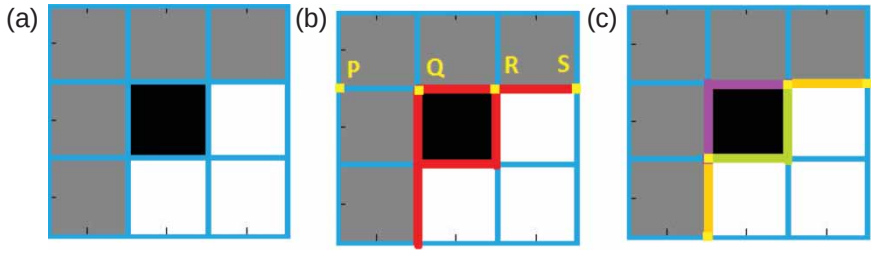

Fig. 3: Example of the classification of the vertices in a discretized layout.

of vertices and polygonal lines, they are mapped from the representation matrix to Cartesian coordinates in the design region.

In order not to modify the topological characteristics of the configuration, the first and the last point in the list are always chosen as control points of the NURBS parameterization, because they are either points touching the boundary of the design region, intersection points or initial and final points on a closed curve. Due to the strong convex hull property of the NURBS, if there are several consecutive control points in a straight line then the elimination of some of them as control points or the choice of a higher degree of the NURBS curve parameterization is recommended in order to have more flexibility and to allow the search for improved shapes in the boundary. The implementation of a routine that performs the automatic choice of the control points with these characteristics is simple.

Once finished the automated process of choosing the control points and the several curves that represent the internal boundaries of the different material regions, the initial values to the weights are chosen as 1 and the knot values are chosen as equally spaced on the interval $(0,1)$ except for the first and last $p+1$ values, where p is the degree of the NURBS curve. The arbitrary choice of values was taken considering that they will be modified by the genetic algorithm when searching for the best values for these parameters. This process will be illustrated ahead in section 2.4 with the study of the optimization of the c-core magnetic actuator.

2.3. Multi-objective Genetic Algorithm

As a final stage of the topology optimization process, the NSGA-II [9] is applied. Figure 4 presents the flowchart of the NSGA-II. The optimization variables in this step are the coordinates of the control points, the weights and the knots of all the NURBS that describe the boundaries. For those control points on the external boundary of the design region, it will be permitted to change its coordinates in a way to stay in the boundary. Concerning the knots, the first and last $p+1$ values are not decision variables, where p is the degree of the NURBS curve. For each variable, lower and upper bounds are defined. The

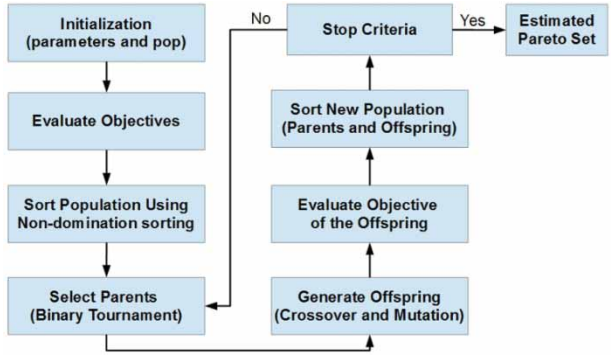

Fig. 4: Flowchart of the NSGA-II.

choice of these values should be made in a way that the topological characteristics are preserved and it is intrinsically related to the problem under study.

2.4. Design of a C-core Magnetic Actuator

The proposed approach was applied to the study of the optimization of a C-core magnetic actuator [2],[5, 6]. The c-core magnetic actuator is composed of three main parts: the armature and the yoke solid blocks of ferromagnetic material; and the design domain, which is discretized into a 20×10 square grid. Each cell within the design domain can assume three states, corresponding to three different materials: air, iron, or a magnetic material (for this specific example, NdFeB magnets were used). The discretization of the c-core actuator design domain is shown in Fig. 5.

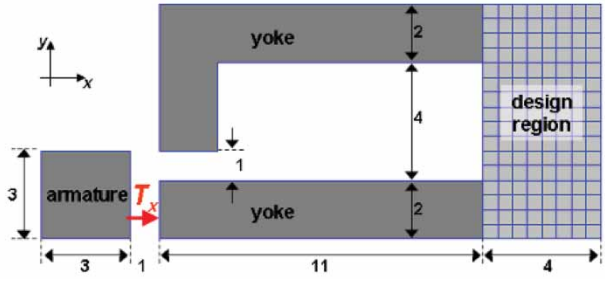

Fig. 5: C-core magnetic actuator (all values are in cm).

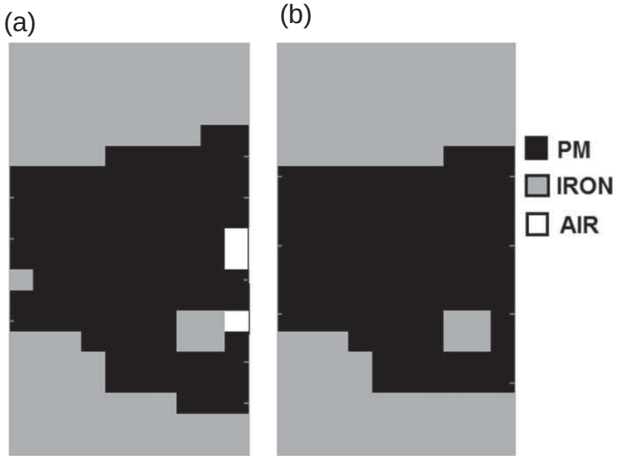

Fig. 6: Layout of the design region: (a) obtained by the MOACO; (b) after the matrix preprocessing.

The multi-objective optimization problem can be stated as:

$$\min_{s\in\Omega} (T_x(s), \mathrm{Vol}_{PM}(s)) \tag{2.5}$$

where T_x is the x-directional attractive force on the armature expressed in terms of the torque, Vol_{PM} is the volume of permanent magnet material (PM) in the design region and Ω is the set of all layouts on the discretized region. The goal of the design is to find an optimal material distribution that maximizes the output torque, or equivalently minimizes the negative of the torque, while minimizing the volume of PM. The cost of the permanent magnet material is related to the volume of PM, and it accounts for the majority part of the cost of the PM machine due to the high price of the rare earth material.

At the first stage of the proposed approach, to solve the problem defined in Eqn. 2.5, the output torque is calculated by FEMM [16] using nonlinear finite element analysis and the algorithm was set up as follows:

- number of ants $n_a = 20$;
- pheromone evaporation rate $\rho = 0.85$;
- $Q = 100$ $\alpha = 1$ and $\tau_{\min} = 0.05$
- maximum number of cycles $nc_{\max} = 1000$

The mask mechanism was applied to $n_t = 10$ topologies from the first front at every $nc_{af} = 25$ cycles. In this case, $t_1 = 20$ masks are randomly applied to each topology, such that at most 10% of the total number of cells is changed in each topology.

Figure 6 (a) shows the layout found by the proposed MOACO that maximizes the attractive force. The maximum found for the force was 950.83 Nm (with percentage of volume of PM equals to 50.5%).

Once the nondominated topologies (estimate of the Pareto front) are obtained, the designer can further analyze specific designs along the set. By choosing one particular point on the estimate of the Pareto front, the parameterization of the boundaries is done as described in section 2.2. Fig. 6(b) shows the topology that maximize the attractive force after

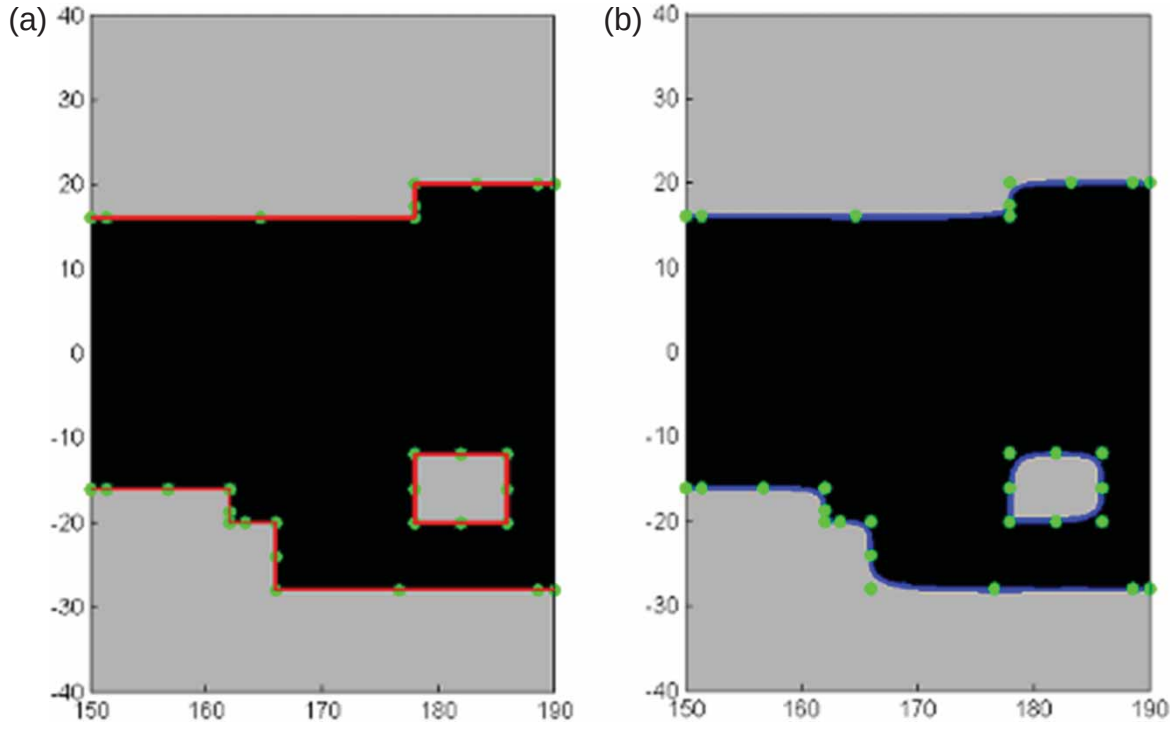

Fig. 7: (a) Polygonal lines boundaries; (b) NURBS curves after parameterization; Control points in green.

the matrix preprocessing. The control points and the polygonal lines obtained from the topology presented in Fig. 6(b) are shown in Fig. 7. After determining the initial knots vector and the weights, this topology, which represents one with maximum torque, is further refined with shape optimization using the NSGA-II.

The NSGA-II was configured with binary tournament to select the parent chromosomes and the genetic operators are the polynomial mutation and the SBX crossover [1]. We adopted the following parameters for the NSGA-II:

- Population size pop = 20;
- Number of generations gen = 50;
- Crossover rate 0.8;
- Pool size equal to half the population size;
- Distribution indices for crossover and mutation operators: both equal 20;
- Lower bound of weights equal to 0 and upper bound equal to 2;
- Range of the coordinates of the control points was equal to half size of the side of the square cell (after matrix refinement);
- For a given knots value its range was half of the distance to its neighbors values;

The suggested choices for the upper and lower bounds for weights, knots and coordinates of the control points were able to maintain the topological properties of the layout. Figure 8 shows the estimated Pareto front (magenta and red points) by MOACO and the improved front for the sample (blue points) selected for parameterization and shape optimization. These results illustrate that the method is capable to improve designs obtained by MOACO in the topology optimization step

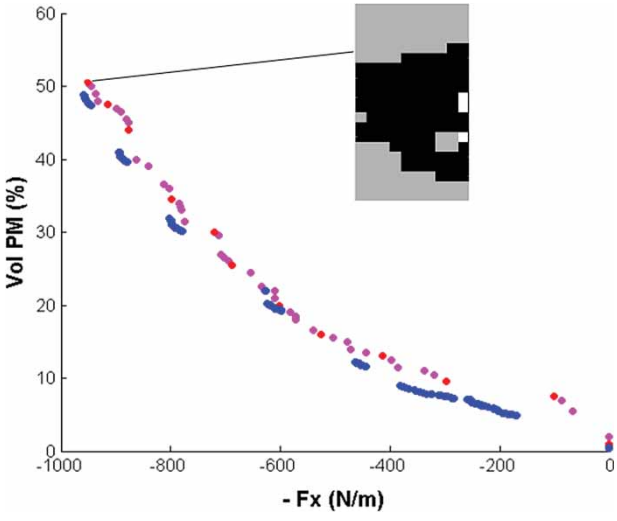

Fig. 8: Estimated Pareto Front (magenta and red points) by MOACO; Samples (red points) selected for parameterization and shape optimization; Estimated Pareto Front (blue points) obtained by NSGA-II from the sample points.

3. CONCLUSION

This work presented a multi-objective approach that integrates topology and shape optimization. This approach is capable to handle problems involving the distribution of several materials in a design domain. The representation used is simple and the results are given in parametric models based on NURBS curves. With a suitable choice of parameters the NSGA-II was capable to improve the results obtained by the MOACO algorithm which shows the adequacy and usefulness of the proposed approach to multi-objective electromagnetic topology optimization. With the proposed approach there is the advantage of finding and providing several solutions of the problem in a single run. In this way, the decision maker can explore a number of alternative designs offered by a multi-objective topology optimization approach. The decision maker can get some insight by analyzing the changes in the shape of the boundary and using the NURBS parameterization to make his/her own changes. Future work include self-adaptive parameters and extension of this approach to 3D problems.

ACKNOWLEDGEMENTS

This research was supported by a Marie Curie International Research Staff Exchange Scheme Fellowship within the 7th European Community Framework Program (FP7) and by the following Brazilian agencies: FAPEMIG [Grants TEC 10018/11, APQ 04611/10], CAPES, CNPq [Grant 312276/2013-3].

REFERENCES

[1] Bandaru, S.; Tulshyan, R.; Deb, K.: Modified SBX and adaptive mutation for real world single objective optimization, 2011 IEEE Congress on Evolutionary Computation (CEC), 1335–1342, 2011. http://dx.doi.org/10.1109/CEC.2011.5949771

[2] Batista, L. S.; Campelo, F.; Guimarães, F. G.; Ramírez, J. A.: Multidomain topology optimization with ant colony systems, COMPEL: The International Journal for Computation and Mathematics in Electrical and Electronic Engineering, 30(6), 2011, 1792–1803. http://dx.doi.org/10.1108/03321641111168101

[3] Batista, L. S.; Li, M.; Campelo, F.; Guimarães, F. G.; Lowther, D. A.; Ramírez, Jaime A.: Ant Colony Optimization for the Topology Design of Interior Permanent Magnet (IPM) Machines, COMPEL: The International Journal for Computation and Mathematics in Electrical and Electronic Engineering, 33(3), 2014, 1–14.

[4] Bendsoe, M. P.; Kikuchi, N.: Generating optimal topologies in structural design using a homogenization method, Computer Methods in Applied Mechanics and Engineering, 71, 1988, 197–224. http://dx.doi.org/10.1016/0045-7825(88)90086-2

[5] Campelo, F.; Ota, S.; Watanabe, K.; Igarashi, H.: Generating parametric design models using information from topology optimization, IEEE Transactions on Magnetics, 44(6), 2008, 986–989. http://dx.doi.org/10.1109/TMAG.2007.916350

[6] Choi, J. S.; Yoo, J.: Simultaneous structural topology optimization of electromagnetic sources and ferromagnetic materials, Computer Methods in Applied Mechanics and Engineering, 198(27–29), 2009, 2111–2121. http://dx.doi.org/10.1016/j.cma.2009.02.015

[7] Cuillière, J-C.; Francois, V.: Integration of CAD, FEA and Topology Optimization through a Unified Topological Model, Computer-Aided Design and Applications, 11(5), 2014, 493–508. http://dx.doi.org/10.1080/16864360.2014.902677

[8] Cuillière, J-C.; Francois, V.; Drouet, J-M.: Towards the Integration of Topology Optimization into the CAD Process, Computer-Aided Design and Applications, 11(2), 2014, 120–140. http://dx.doi.org/10.1080/16864360.2014.846067

[9] Deb, K.; Pratap, A.; Agarwal, S.; Meyarivan, T.: A fast and elitist multiobjective genetic algorithm: NSGA-II, Trans. Evol. Comp, 6(2), 2002, 182–197. http://dx.doi.org/10.1109/4235.996017

[10] Dorigo, M.; Blum, C.: Ant colony optimization theory: A survey, Theoretical Computer Science, 344 (2–3), 2005, 243–278. http://dx.doi.org/10.1016/j.tcs.2005.05.020

[11] Heo, S. H.; Baek, M. K.; Lee, K. H.; Hong, S. G.; Park, I. H.: Shape and topology optimization of rotor in synchronous reluctance motor using continuum sensitivity and adaptive level set method, International Conference on Electrical Machines and Systems (ICEMS), 2013, 129–133.

[12] Hongwei, Z.; Xiaokai, C.; Yi, L.; Mingjun, Z.: Topology optimization for air suspension bracket integrated shape optimization, IEEE Vehicle Power and Propulsion Conference, 2008 1–5, VPPC '08.

[13] Kim, Y. S.; Park, I. H.: Topology Optimization of Rotor in Synchronous Reluctance Motor Using Level Set Method and Shape Design Sensitivity, IEEE Transactions on Applied Superconductivity, 20(3), 2010, 1093–1096. http://dx.doi.org/10.1109/TASC.2010.2040725

[14] Larsen, S.; Jensen, C. G.: Converting topology optimization results into parametric CAD models, Computer-Aided Design & Applications, 6(3), 2009, 407–418. http://dx.doi.org/10.3722/cadaps.2009.407-418

[15] Lin, C.-Y.; Chao, L.-S.: Automated image interpretation for integrated topology and shape optimization, Structural and Multidisciplinary Optimization, 20(2), 2000, 125–137. http://dx.doi.org/10.1007/s001580050144

[16] Meeker, D.: Finite Element Method Magnetics, Version 4.2 User's Manual, 2010. Online acess: http://www.femm.info

[17] Robinson, T. T.; Armstrong, C. G.; Chua, H. S.; Othmer, C.; Grahs, T.: Optimizing Parameterized CAD Geometries Using Sensitivities Based on Adjoint Functions, Computer-Aided Design and Applications, 9(3), 2012, 253–268. http://dx.doi.org/10.3722/cadaps.2012.253-268

[18] Takahashi, N.; Yamada, T.; Miyagi, D.: Examination of optimal design of IPM motor using ON/OFF method, IEEE Transactions on Magnetics, 46(8), 2010, 3149–3152. http://dx.doi.org/10.1109/TMAG.2010.2044382

[19] Tang, P.-S.; Chang, K.-H.: Integration of topology and shape optimization for design of structural components, Structural and Multidisciplinary Optimization, 22(1), 2001, 65–82. http://dx.doi.org/10.1007/PL00013282

[20] Zhou, A.; Qu, B. Y.; Li, H.; Zhao, S. Z.; Suganthan, P. N.; Zhang, Q.: Multiobjective evolutionary algorithms: A survey of the state of the art, Swarm and Evolutionary Computation, 1(1), 2011, 32–49. http://dx.doi.org/10.1016/j.swevo.2011.03.001